

## **HMGB1 coordinates SASP-related chromatin folding and RNA homeostasis on the path to senescence**

Konstantinos Sofiadis<sup>1,#</sup>, Milos Nikolic<sup>2,#</sup>, Yulia Kargapolova<sup>2</sup>, Natasa Josipovic<sup>1</sup>, Anne Zirkel<sup>2</sup>, Antonis Papadakis<sup>3</sup>, Ioanna Papadionysiou<sup>1</sup>, Gary Loughran<sup>4</sup>, James Keane<sup>4,5</sup>, Audrey Michel<sup>4</sup>, Eduardo G. Gusmao<sup>1</sup>, Athanasia Mizi<sup>1</sup>, Theodore Georgomanolis<sup>2,6</sup>, Janine Altmüller<sup>6</sup>, Peter Nürnberg<sup>6</sup>, Andreas Beyer<sup>3</sup> & Argyris Papantonis<sup>1,2,\*</sup>

<sup>1</sup>*Institute of Pathology, University Medical Center Göttingen, 37075 Göttingen, Germany*

<sup>2</sup>*Center for Molecular Medicine Cologne, University of Cologne, 50931 Cologne, Germany*

<sup>3</sup>*Cluster of Excellence Cologne for Age-associated Disease, University of Cologne, 50931 Cologne, Germany*

<sup>4</sup>*Ribomaps, Western Gateway Building, T12 XF62 Cork, Ireland*

<sup>5</sup>*Cork Institute of Technology, T12 P928 Cork, Ireland*

<sup>6</sup>*Cologne Center for Genomics, University of Cologne, 50931 Cologne, Germany*

<sup>#</sup>These authors contributed equally to this work

\*Corresponding author; Tel.: +49 551 39 65734, Email: [argyris.papantonis@med.uni-goettingen.de](mailto:argyris.papantonis@med.uni-goettingen.de)

This **Supplemental Material** contains **Figures S1-S7** and **Tables S1-S5**.

## Supplemental Figures

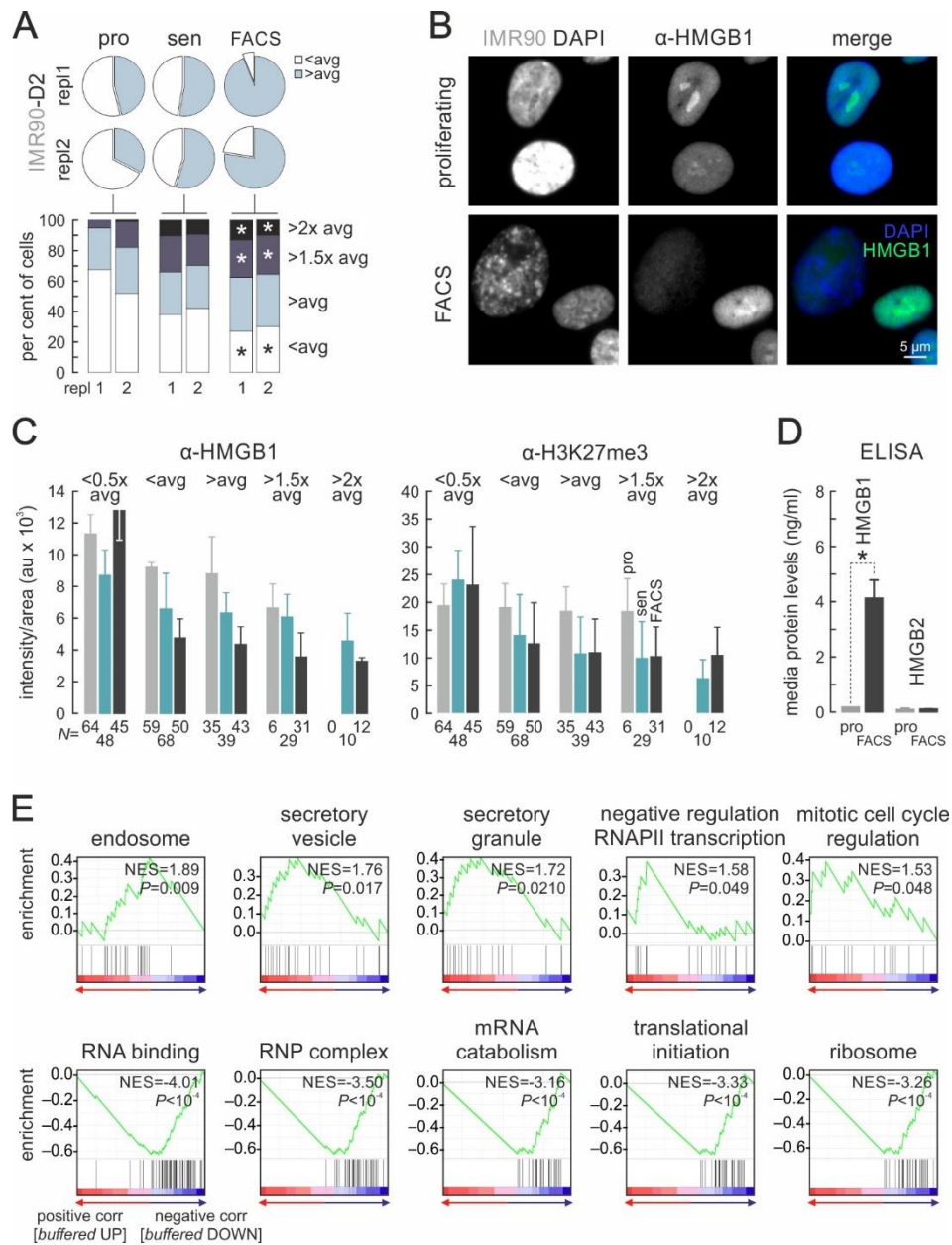


**Figure S1. HMGB1 depletion occurs in enlarged nuclei and is marked by gene expression changes.**

- (A) Pie charts (*top*) showing senescent IMR90 populations containing larger-than-average cell nuclei, which can be enriched via FACS. Bar graphs (*bottom*) show stratification of cells according to increasing nuclear size (compared to the population average). \*: significantly different to proliferating cells,  $P < 0.05$ ; Fisher's exact test.
- (B) Representative images of proliferating (*top row*) and FACS-sorted senescent IMR90 (*bottom row*) immunostained for HMGB1 and counterstained by DAPI. Bar: 5  $\mu\text{m}$ .
- (C) Bar graphs showing declining HMGB1 (*left*) and H3K27me3 levels (mean  $\pm$  S.D.; *right*) in proliferating (*grey*), senescent (*green*) and FACS-sorted IMR90 (*black*) stratified according to nuclear size from images like those in panel B. The number of cells analyzed in each subgroup ( $N$ ) is indicated.

- (D) Bar graphs showing HMGB1/B2 levels (mean  $\pm$  S.D.) detected in the growth media of proliferating (*grey*) or FACS-sorted IMR90 (*black*). \*:  $P < 0.01$ ; unpaired two-tailed Student's t-test ( $N=2$ ).
- (E) Gene set enrichment analysis (GSEA) of genes whose expression is “buffered” in Ribo-seq data. Normalized enrichment scores (NES) and associated  $P$ -values for each set are shown.

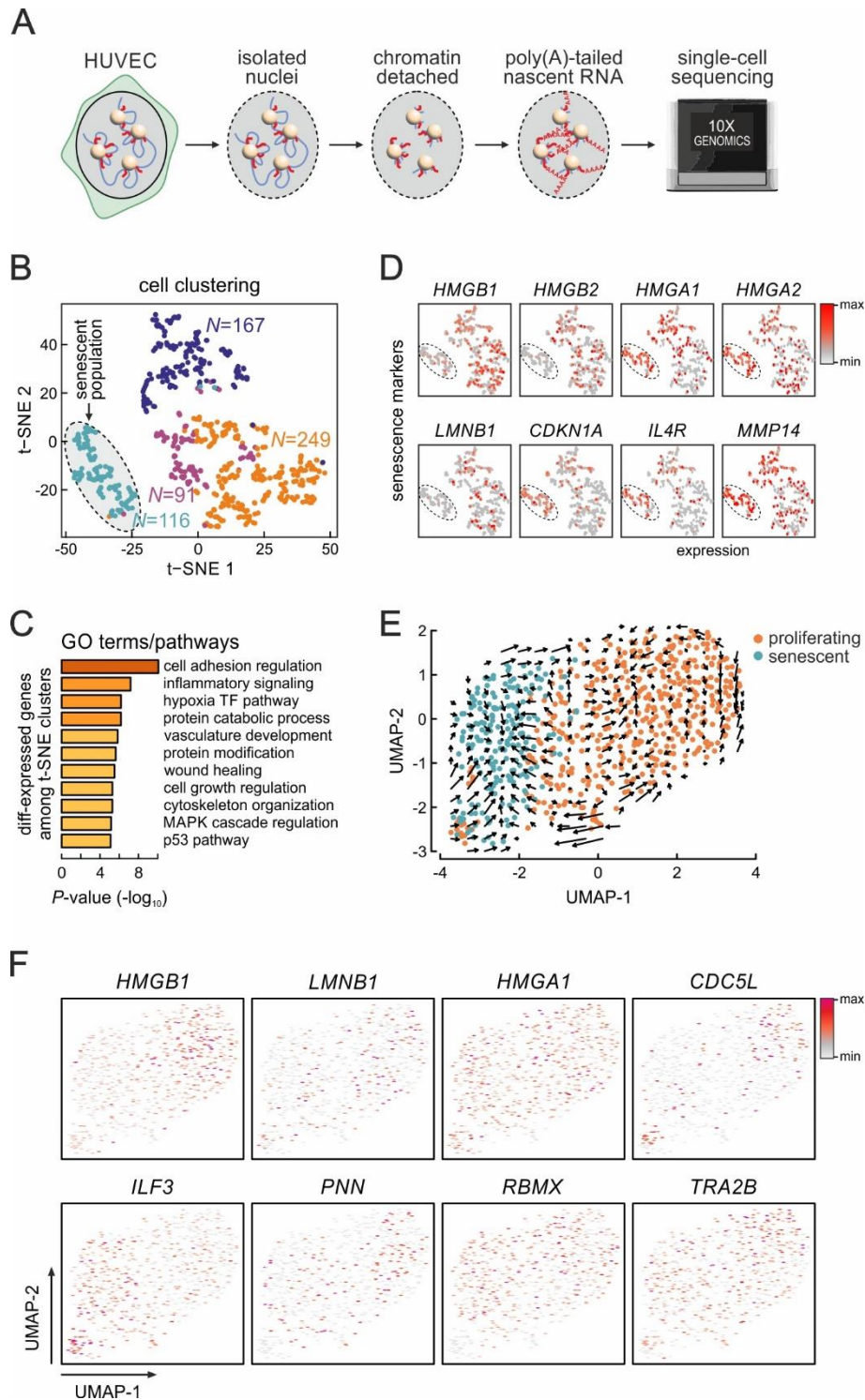


**Figure S2. Single-cell sequencing of nascent RNA.**

- (A) Strategy for nascent scRNA-seq involving isolation of intact HUVEC nuclei, detachment of non-transcribed chromatin (blue) via DNase I digestion, and *in situ* polyadenylation of nascent RNA (red) at transcription foci (spheres), before standard processing on a 10X Genomics platform.
- (B) t-SNE clustering of data from 623 nuclei separates three proliferating cell groups (blue, red, purple, and green) from the senescent ones (grey oval);  $N$  indicates the number of cells per cluster.
- (C) Bar graphs showing  $(-\log)$  enrichment  $P$ -values for GO terms associated with differentially-expressed genes amongst the clusters from panel B.

- (D) Heatmaps showing normalized expression levels of selected senescence marker genes in individual cells clustered as in panel B.
- (E) UMAP reduction plot showing results from *Velocity* analysis. Arrows indicate trajectories of proliferating HUVECs (*orange*) towards senescent ones (*green*) based on unspliced/spliced RNA ratios in individual cells.
- (F) Heatmaps showing normalized expression levels of selected genes in individual cells clustered as in panel E.

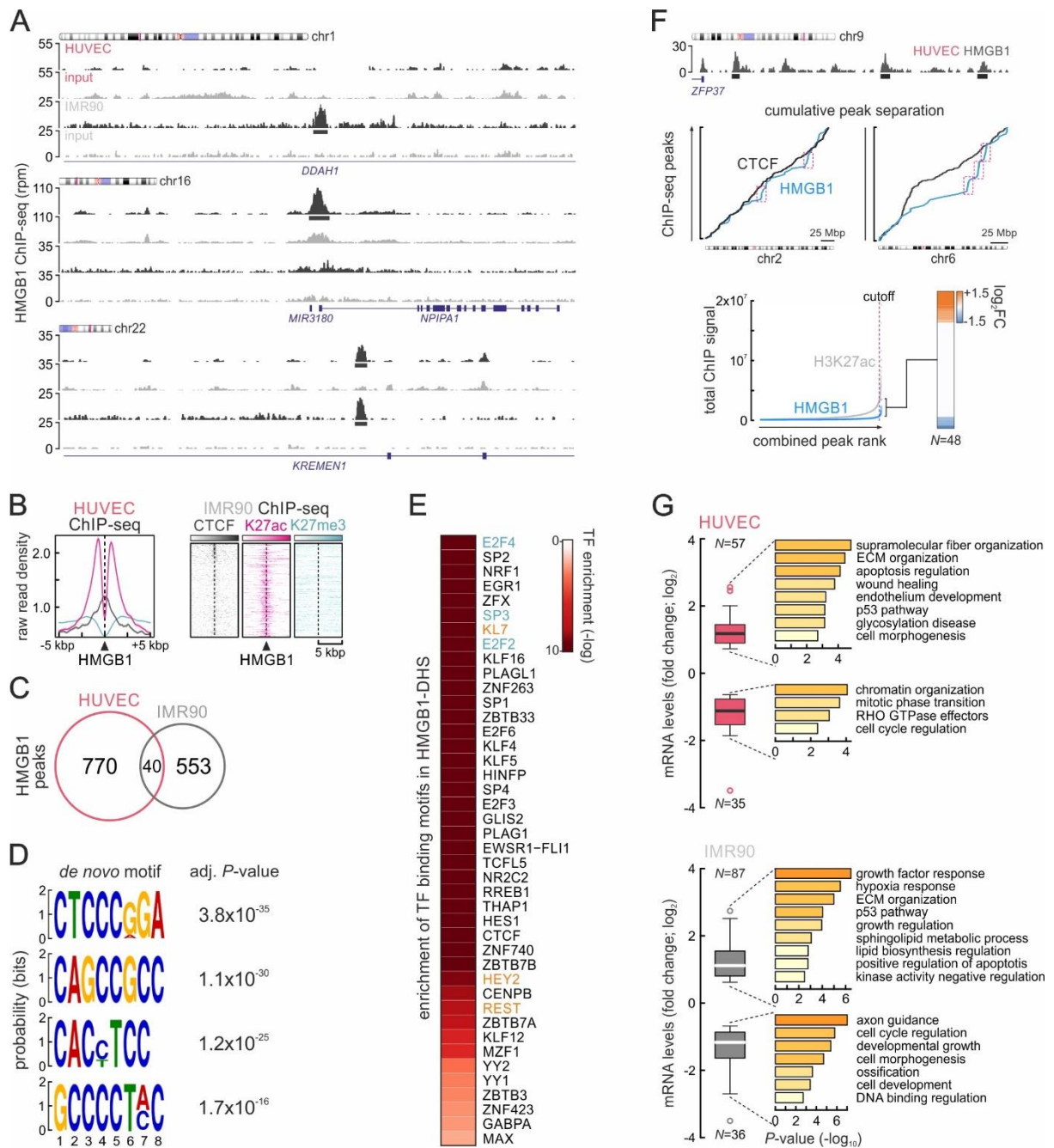


**Figure S3. HMGB1 chromatin-binding features in proliferating cells.**

- (A) Genome browser views showing raw HMGB1 ChIP-seq signal at loci in chr1, 16, and 22 from both HUVEC and IMR90 (black); input tracks (grey) provide a control.
- (B) Line plots and heat maps showing distribution of H3K27ac (magenta), H3K27me3 (light blue), and CTCF ChIP-seq signal (grey) in the 20 kbp around HMGB1 peaks from HUVECs and IMR90, respectively.
- (C) Venn diagrams showing minimal overlap between HMGB1 binding peaks from HUVEC and IMR90. Overlap is not more than what is expected by chance;  $P > 0.1$ , Chi-square Goodness-of-Fit test.
- (D) Logos and associated adjusted  $P$ -values for the most enriched *de novo* motifs discovered in DNase I-accessible footprints under HMGB1 peaks.
- (E) Heatmap showing most enriched TF binding motifs in the footprints from panel C; up- ( $>0.6 \log_2$ -fold change; orange) or downregulated TFs ( $<-0.6 \log_2$ -fold change; green) are indicated.

- (F) Genome browser views (*top*) showing clustered HMGB1 ChIP-seq peaks (*black boxes*) near the ZFP37 gene promoter on HUVEC chr9. Plots (*middle*) showing the cumulative distribution of HMGB1 ChIP-seq peaks along HUVEC chr2, 6 and 9 (*green*); CTCF peak distributions (*black*) provide a control. Plot (*bottom left*) ranking “stitched” H3K27ac-marked enhancers (*grey*) and HMGB1-bound sites; those over the cutoff (*magenta*) qualify as “superenhancers”. mRNA fold-changes ( $\log_2$ ) of the 48 genes linked to HMGB1 “superenhancers” are plotted as a heatmap (*bottom right*).
- (G) Box plots showing mRNA fold-changes ( $\log_2$ ) of genes differentially-expressed upon senescence and bound by HMGB1 in HUVECs (*top*) and IMR90 (*bottom*). GO terms associated with each subgroup and their enrichment *P*-values are shown. The number of genes in each group (*N*) is indicated.



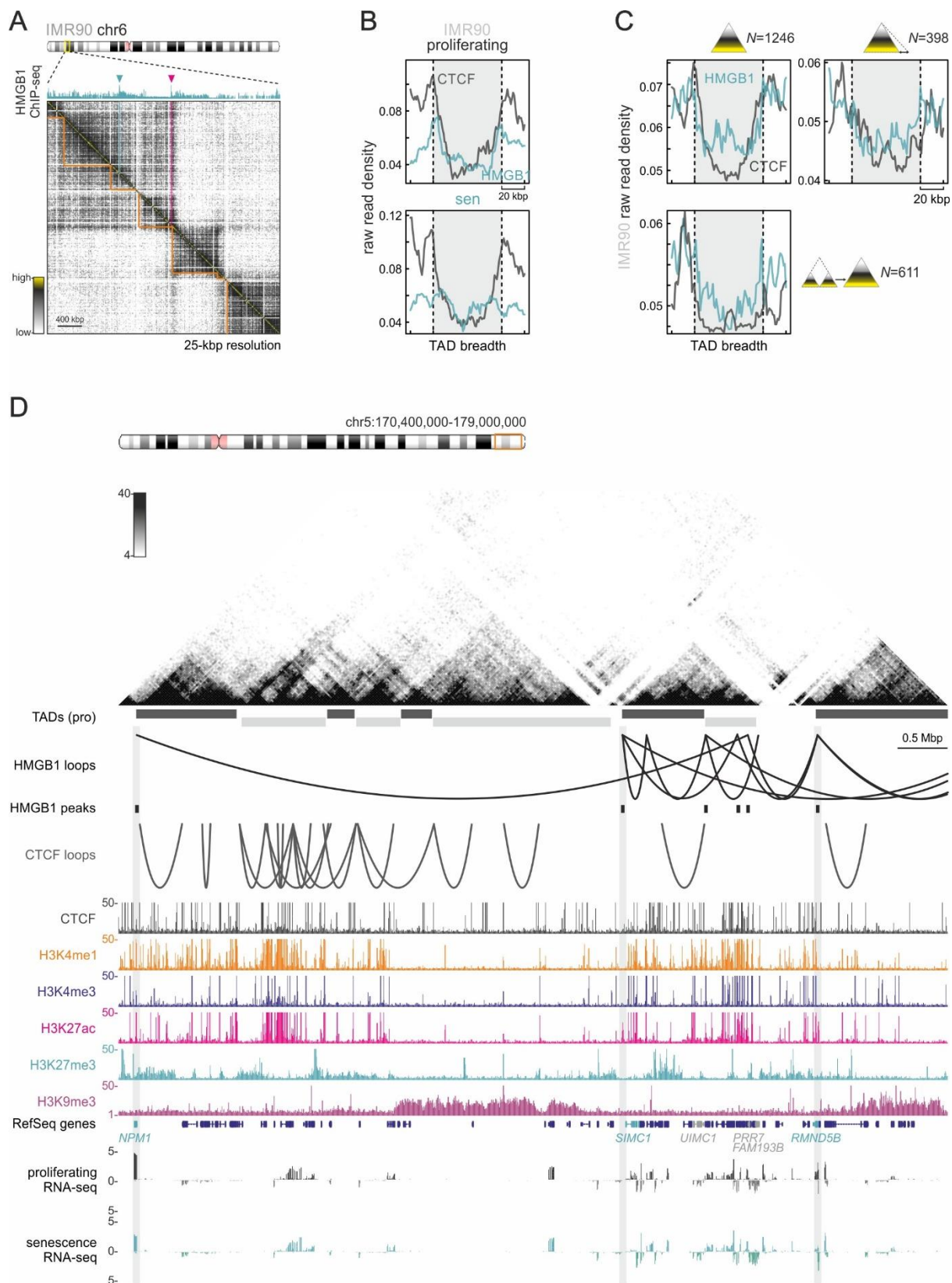


**Figure S4. HMGB1 demarcates TAD boundaries in proliferating IMR90 and HUVECs.**

(A) Exemplary Hi-C heatmap for a subregion in IMR90 chr6 aligned to HMGB1 ChIP-seq; peaks at TAD boundaries (*orange lines*) are indicated (*magenta arrowheads*).



- (B) Line plots showing average HMGB1 (*green*) and CTCF ChIP-seq profiles (*grey*) along TADs  $\pm 20$  kbp from proliferating (*top*) or senescent IMR90 (*bottom*).
- (C) As in panel F, but for TADs that do not change (*top left*), shift one boundary (*top right*) or merge upon senescence entry (*bottom left*). *N* indicates the number of TADs in each subgroup.
- (D) Exemplary Hi-C data (25-kbp resolution) in an 8.6-Mbp region of HUVEC chr5 aligned to positions of TADs, HMGB1 and CTCF loops, as well as to ENCODE ChIP-seq and own RNA-seq data. The positions of HMGB1 peaks at downregulated promoters (*green gene names*) are highlighted (*grey*).

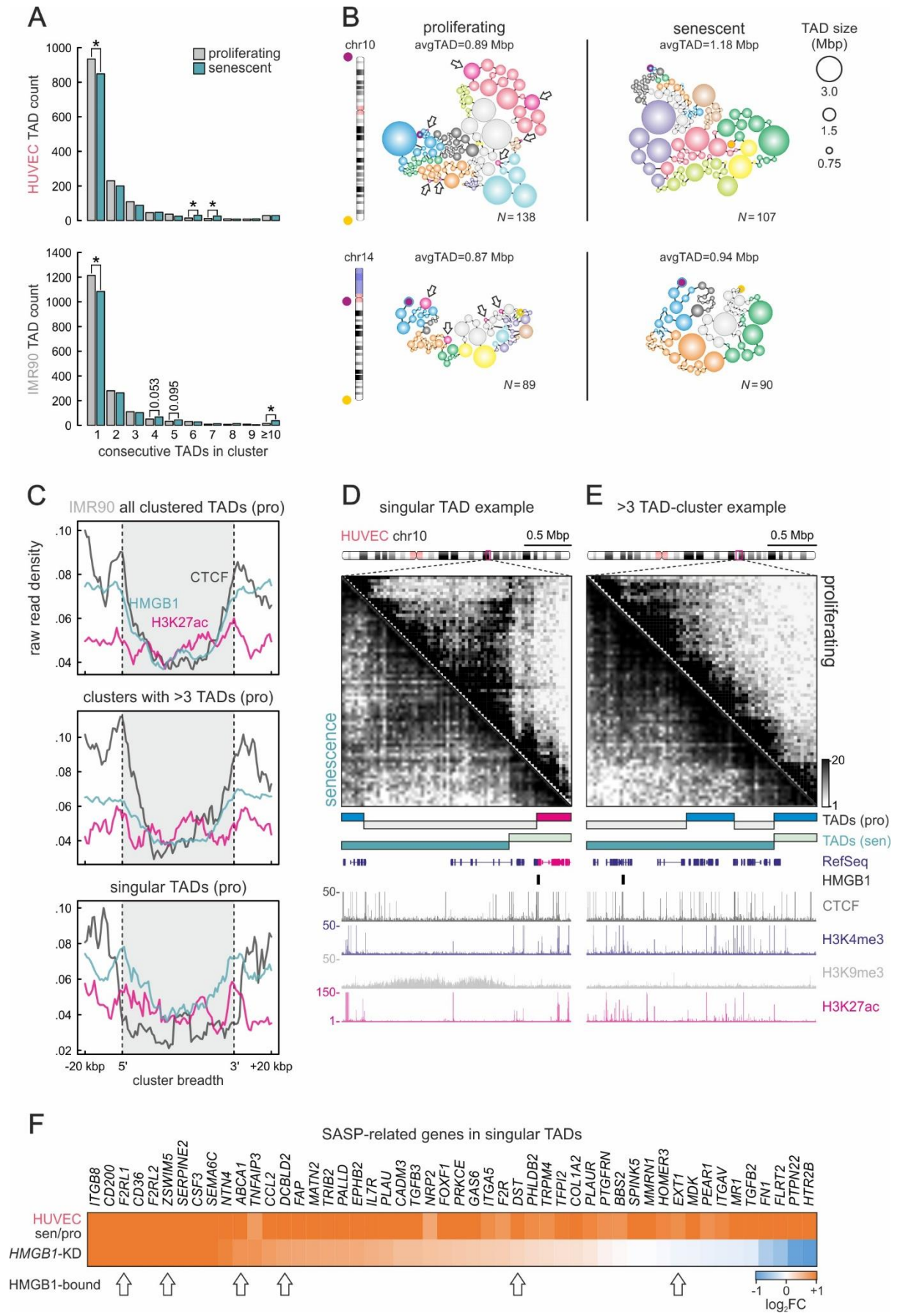


**Figure S5. HMGB1 demarcates specific TAD subsets in primary human cells.**

- (A) Bar plots showing the number of TADs contained in progressively larger clusters derived using TiLO on proliferating (*grey*) and senescent Hi-C data (*green*) from HUVEC (*top*) and IMR90 (*bottom*). \*:  $P < 0.01$ ; Fisher's exact test.
- (B) Illustration of TAD clusters identified using proliferating (*left*) and senescent HUVEC Hi-C data (*right*) for chr10 and 14. Spheres represent TADs; the most 5'/3' TADs (*purple* and *yellow dots*, respectively) and "singular" TADs (*arrows*) are indicated.
- (C) Line plots showing average HMGB1 (*green*), CTCF (*grey*), and H3K27ac ChIP-seq profiles (*magenta*) at the extremities of all clustered TADs ( $\pm 20$  kbp; *top*), of clusters of  $>3$  TADs (*middle*) or of "singular" TADs (*bottom*) from proliferating IMR90.
- (D) Exemplary Hi-C data (40-kbp resolution) around a "singular" TAD (*magenta*) in HUVEC chr10 aligned to TAD positions, HMGB1 peaks, and ENCODE ChIP-seq.
- (E) As in panel D, but for TADs that form a  $>3$ -TAD cluster in TiLO data.
- (F) Heatmap showing senescence-induced changes in expression levels ( $\log_2$ FC) of SASP-related genes embedded in singular TADs like those in panel B. Genes bound by HMGB1 are indicated (arrows), and are not more than what would be expected by chance;  $P > 0.1$ , Chi-square Goodness-of-Fit test.

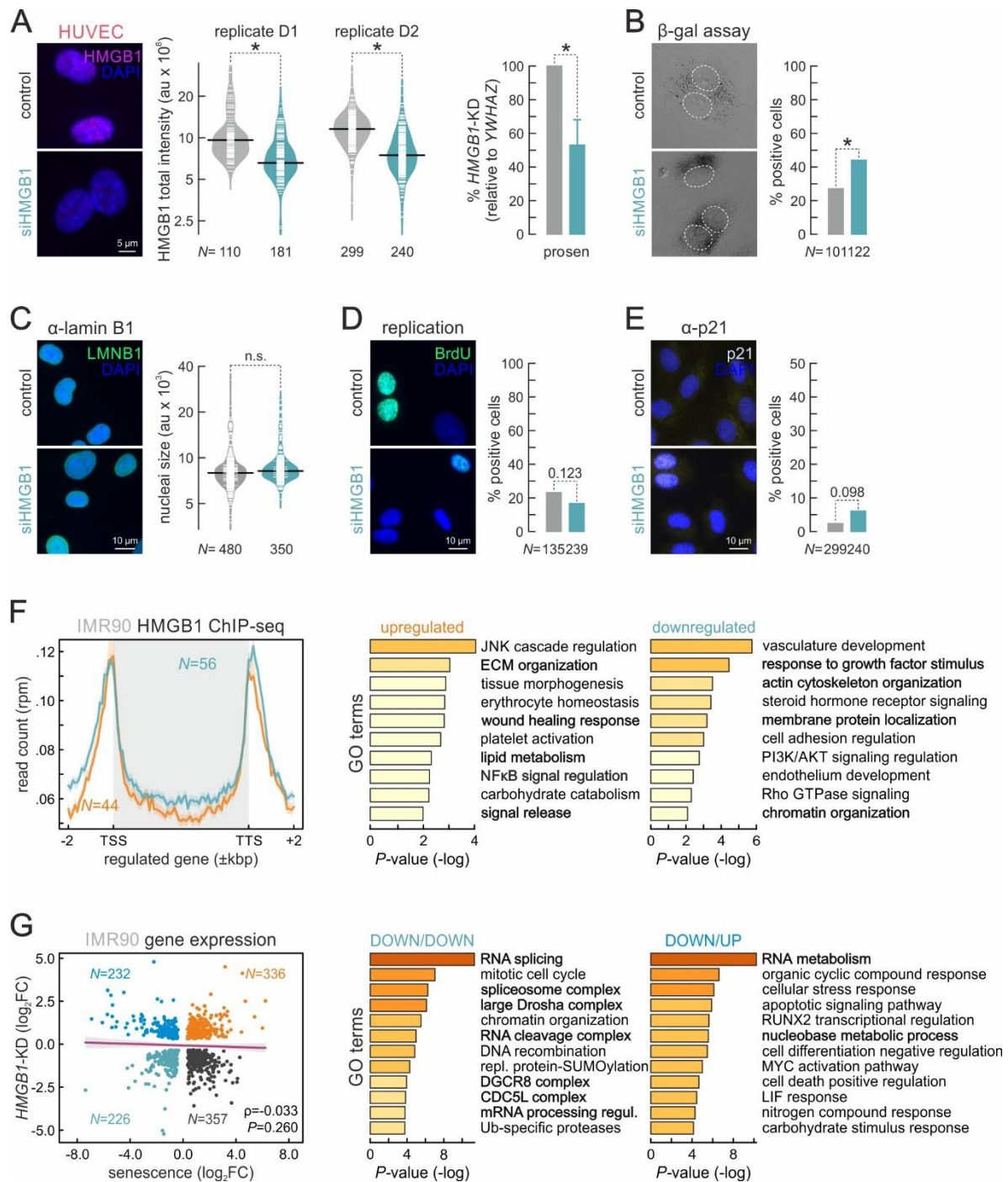


**Figure S6. Effects of *HMGB1* knockdown in proliferating HUVECs and IMR90.**

- (A) Representative immunofluorescence images of siHMGB1-treated HUVECs showing reduced HMGB1 levels compared to control cells (*left*). Bean plots quantify knockdown efficiency (*middle*; *N* indicates the number of cells analyzed). Bar graphs (*right*) show normalized *HMGB1* mRNA levels ( $\pm$  S.D.; *N*=2) in knockdown compared to control cells. Bar: 5  $\mu$ m. \*: *P*<0.01; Wilcoxon-Mann-Whitney and unpaired two-tailed Student's t-test for bean and bar plots, respectively.
- (B) Representative brightfield images of siHMGB1-treated HUVECs showing elevated  $\beta$ -galactosidase activity compared to control cells (*left*); bar graphs quantify this increase (*right*; *N* indicates the number of cells analyzed). \*: *P*<0.01; Fisher's exact test.

- (C) As in panel A, but for LMNB1 levels. Bar: 10  $\mu$ m. No statistically significant difference (n.s.); Wilcoxon-Mann-Whitney test.
- (D) As in panel A, but for BrdU incorporation. Bar: 10  $\mu$ m.  $P=0.123$ ; Fisher's exact test.
- (E) As in panel A, but for p21 levels. Bar: 10  $\mu$ m.  $P=0.098$ ; Fisher's exact test.
- (F) Line plots (*left*) showing average HMGB1 ChIP-seq profiles along genes up- (*orange*) or downregulated upon *HMGB1*-knockdown in IMR90 (*green*;  $N$  indicates the number of directly HMGB1-bound genes). Bar plots (*middle/right*) showing GO terms associated with either gene set and their enrichment  $P$ -values; terms relevant to senescence are highlighted (*black*).
- (G) Scatter plots (*left*) showing correlation between differentially-expressed genes ( $\log_2FC$ ) upon senescence entry and *HMGB1*-knockdown in IMR90. The Pearson's correlation ( $\rho$ ) and its associated  $P$ -value are shown alongside the number of genes ( $N$ ) in each subgroup. Bar plots (*middle/right*) showing GO terms and enrichment  $P$ -values associated with genes commonly downregulated ("DOWN/DOWN") or downregulated in senescence but upregulated upon *HMGB1*-knockdown ("DOWN/UP"); terms relevant to RNA processing are highlighted (*black*).

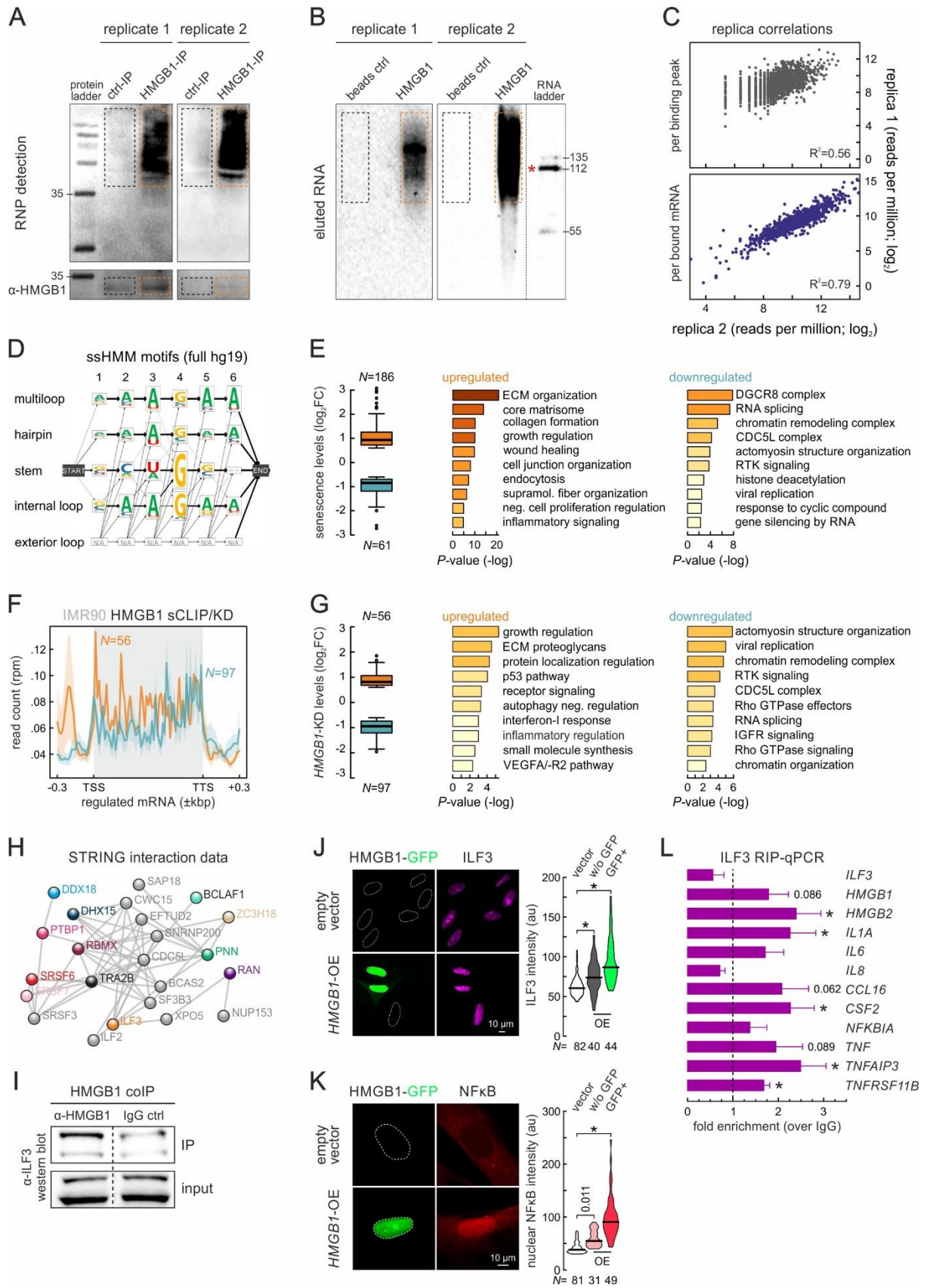




**Figure S7. HMGB1 sCLIP controls and analysis of HMGB1-interacting RBPs.**

- (A) Electrophoretic profiles of control (beads only; *black dotted square*) and HMGB1 IP (*orange dotted rectangle*) probed for RNA (*top*) or the HMGB1 protein (*bottom*) in both sCLIP replicates. The 35-kDa band of the molecular mass ladder is indicated.
- (B) Electrophoretic profiles of RNA eluted from control (beads only; *black dotted square*) or HMGB1 IP (*orange dotted rectangle*) in both sCLIP replicates. The 112-nt band of the molecular mass ladder is indicated (*red star*) and corresponds to ~144 pg of RNA.
- (C) Scatter plots showing correlation of sCLIP data from two independent biological replicates compared per binding peak (*top*) or per bound mRNA normalized read count (*bottom*). Spearman correlation values ( $R^2$ ) are indicated.
- (D) Output of ssHMM motif analysis of sCLIP data showing sequence probabilities in HMGB1-bound motifs predicted to form different structures using the reference human genome (hg19).
- (E) Box plots (*left*) showing expression fold-changes ( $\log_2$ ) of mRNAs differentially-regulated upon senescence and bound by HMGB1 in IMR90 sCLIP. The number of peaks ( $N$ ) analyzed is indicated below each bar. Bar graphs (*right*) with GO terms associated with each subgroup and their enrichment  $P$ -values are also shown.
- (F) Line plots (*left*) showing average HMGB1 sCLIP profiles along mRNAs up- (*orange*) or downregulated upon *HMGB1*-knockdown in IMR90 (*green*;  $N$  indicates the number of directly HMGB1-bound genes).
- (G) As in panel E, but for the up-/downregulated genes from panel F.
- (H) Experimentally-validated protein-protein interaction network for HMGB1 co-immunoprecipitating RBPs (*colored spheres*) that are also downregulated in senescence. Their secondary interactors (*grey spheres*) from the STRING database are also shown.
- (I) Western blots using antisera recognizing ILF3 on proteins co-immunoprecipitating with HMGB1 (*left*) or IgG (*right*) in IMR90; blots on 10% of input material provides a loading control.
- (J) Representative images of IMR90 overexpressing HMGB1-GFP and immunostained for ILF3. Nuclear outlines are indicated (*dashed lines* based on DAPI counterstaining). IMR90 transfected with empty vectors provide a control. Bar: 10  $\mu\text{m}$ . Signal intensities are quantified in the violin plots (*right*). \*: significantly different to control;  $P < 0.001$ , Wilcoxon-Mann-Whitney test
- (K) As in panel I, but immunostained for phospho-NF $\kappa$ B. Bar: 10  $\mu\text{m}$ .
- (L) Bar graphs showing mean fold-enrichments (over IgG controls  $\pm$ S.D.,  $N=2$ ) of selected mRNAs from ILF3 RIP experiments in proliferating IMR90. \*: significantly different to control;  $P < 0.05$ , unpaired two-tailed Student's  $t$ -test

**Supplemental Table Legends** (tables are provided as .xlsx files online)

**Table S1. HMGB1 sCLIP target mRNAs.** List of high-confidence HMGB1-bound mRNAs from two sCLIP biological replicates.

**Table S2. HMGB1 ChIP-seq peaks and long-range loops.** List of high confidence HMGB1 ChIP-seq peaks from (A) proliferating HUVEC and (B) proliferating IMR90. (C) List of intrachromosomal HMGB1 long-range loops from proliferating HUVEC.

**Table S3. Differentially-expressed genes.** Differentially-expressed genes between (A) all clusters in single cell nascent RNA-seq data; (B) proliferating and senescent HUVEC; (C) proliferating and senescent IMR90; (D) control and *HMGB1*-knockdown IMR90.

**Table S4. HMGB1 interacting proteins.** Full list of proteins (A) co-immunoprecipitating with HMGB1 (significant ones highlighted in bold), alongside a summary of the biological replicates submitted, and the technical parameters of the proteomics run; (B) recovered by whole-cell proteomics comparing proliferating to senescent IMR90.

**Table S5. Ribo-seq data analysis.** Full list of genes tested in Ribo-seq (performed in biological triplicates) alongside their total RNA, translation, and buffering indexes.